

# Molecular Dynamics Simulation of Dissociation Kinetics

Andrew L. Kantor,\* Lyle N. Long,<sup>†</sup> and Michael M. Micci<sup>†</sup>  
Pennsylvania State University, University Park, Pennsylvania 16802

The vibrational energy distribution and the degree of dissociation within a system of hydrogen or oxygen molecules were modeled using molecular dynamics. The first step in this process was to model the atomic and molecular interactions. Because hydrogen and oxygen form diatomic molecules, vibration is the only intramolecular force that must be computed. The Morse potential (Morse, P. M., "Diatomic Molecules According to the Wave Mechanics. II. Vibration Levels," *Physical Review*, Vol. 34, July 1929, pp. 57–64) is used to perform this calculation. Atomic interactions outside the molecule are modeled using the Lennard–Jones potential. The vibrational energy level distribution of this model demonstrated excellent agreement with the Boltzmann distribution. In this molecular dynamics simulation, dissociation occurs when the potential energy between two vibrating atoms exceeds a critical value. Recombination is also possible between two previously dissociated atoms by the reverse mechanism. This process enables a system to start in a state of molecules and proceed to an equilibrated state of atoms and molecules. The molecular dynamics simulation accurately modeled both the rate of dissociation and the ratio of species at equilibrium. This investigation demonstrated that simple chemical reactions in relatively large systems can be modeled using molecular dynamics.

## Nomenclature

$\mathbf{a}$	= acceleration vector
$C_f$	= reaction rate parameter
$D$	= dissociation energy
$E_\infty$	= Morse parameter <sup>5</sup>
$f$	= intermolecular force
$g_l$	= degeneracy
$H$	= Hamiltonian
$h$	= Planck's constant
$k$	= Boltzmann constant
$L$	= Lagrangian
$m$	= atomic mass
$N$	= number of molecules
$N^*$	= number of molecules in a particular energy level
$n$	= reaction rate parameter
$p$	= momentum
$Q_{el}^a$	= atomic electronic partition function
$Q_{el}^{aa}$	= molecular electronic partition function
$q$	= generalized coordinates
$r$	= internuclear separation
$r_e$	= mean bond length
$r_{ij}$	= distance between atoms $i$ and $j$
$T$	= temperature
$t$	= time
$u$	= intermolecular potential
$V$	= intramolecular potential
$\mathbf{v}$	= velocity vector
$x_e\omega_e$	= first anharmonic correction
$\alpha$	= degree of dissociation
$\alpha^*$	= equilibrium degree of dissociation
$\beta$	= Morse parameter <sup>5</sup>
$\varepsilon$	= Lennard–Jones energy parameter
$\varepsilon_v$	= vibrational energy
$\theta_d$	= characteristic dissociation temperature
$\theta_r$	= rotational characteristic temperature

$\theta_v$	= vibrational characteristic temperature
$v$	= quantum energy level
$\rho$	= density
$\rho_d$	= characteristic density
$\sigma$	= Lennard–Jones size parameter
$\omega_e$	= spacing of vibrational energy levels

## Introduction

**M**OLECULAR dynamics (MD) has recently been utilized to simulate liquid oxygen droplet vaporization in a supercritical hydrogen environment.<sup>1</sup> The advantages of using MD include the elimination of the requirement to track phase boundaries (when they exist), the need to include a priori a high-pressure equation of state, and material and transport properties over a wide range of temperatures and pressures. The MD simulations clearly showed the disappearance of surface tension at the critical point and mixture effects on the critical pressure and temperature. Results remained the same as system sizes were varied by more than an order of magnitude. MD simulations have also been used to calculate high-pressure and temperature transport properties and equations of state with excellent agreement to experimentally measured values.<sup>2,3</sup>

These previous studies only included translational and rotational energy storage for the molecular species due to the relatively low (<300 K) gaseous environment temperatures. To extend this work to temperatures representative of liquid rocket combustion chambers, vibrational energy storage and possible dissociation must be included. Thus, the purpose of this study was to add vibrational energy storage and dissociation to the MD simulation of supercritical oxygen and hydrogen.

## MD

MD is the numerical simulation of atomic and molecular motions and forces in a system. When the trajectories of these particles are observed, many thermodynamic and fluid mechanical properties can be calculated. The main advantage of this technique is that its accuracy is only dependent on the selection of an intermolecular potential and the precision of the numerical integrator. No physical properties need to be known nor assumptions made about the simulated medium. However, the disadvantage is that the size of the molecular systems must be extremely small. This is due to the large number of force calculations that must be made.

Modeling the atomic potentials is one of the most important parts of an MD simulation. This particular investigation deals with atoms that are free to vibrate within the molecules. Such a system requires both intermolecular and intramolecular potentials. The

Presented as Paper 2000-0213 at the AIAA 38th Aerospace Sciences Meeting, Reno, NV, 10–13 January 2000; received 10 November 2000; revision received 23 April 2001; accepted for publication 24 April 2001. Copyright © 2001 by the American Institute of Aeronautics and Astronautics, Inc. All rights reserved.

\*Graduate Research Assistant, Department of Aerospace Engineering, Student Member AIAA.

<sup>†</sup>Professor, Department of Aerospace Engineering, Associate Fellow AIAA.

intramolecular potential is utilized in computing the forces between two atoms of the same molecule, whereas the intermolecular potential is used to calculate forces between atoms of different molecules.

### Intermolecular Potential

In MD the potential is taken to be pairwise additive. This means that the total energy in the system is a sum of the isolated two-body contributions. Three-body and higher terms are usually neglected because of the vast increase in computational time and their relatively small influence on gaseous systems. The most commonly used pairwise additive potential  $u$  for modeling intermolecular forces between atoms separated by a distance  $r_{ij}$  is the one proposed by Lennard-Jones (see Ref. 4),

$$u(r_{ij}) = 4\epsilon \left[ (\sigma/r_{ij})^{12} - (\sigma/r_{ij})^6 \right] \quad (1)$$

This potential produces a short-range atomic repulsion that simulates the overlap of electron clouds and a long-range attraction due to induced dipoles. The only adjustable parameters are a size parameter  $\sigma$  and an energy parameter  $\epsilon$ . Both of these values are a function of the species being simulated. Because the intermolecular forces are necessarily conservative, the force resulting from the preceding potential is

$$f(r) = -\frac{du(r)}{dr} = 24\frac{\epsilon}{\sigma} \left[ 2\left(\frac{\sigma}{r_{ij}}\right)^{13} - \left(\frac{\sigma}{r_{ij}}\right)^7 \right] \quad (2)$$

### Intramolecular Potential

The potential between two atoms of the same molecule differs slightly from the intermolecular potential. To conform to spectroscopic experiments, the intramolecular potential is required to have a potential well at the mean bond length and approach the dissociation energy as the atoms become infinitely separated. In addition, like the Lennard-Jones potential, it must go to infinity as the atoms approach each other. One such model that conforms to these specifications is the Morse potential.<sup>5</sup> This potential is given by

$$V(r) = De^{-2\beta(r-r_e)} - 2De^{-\beta(r-r_e)} + E_\infty \quad (3)$$

where  $\beta$  and  $E_\infty$  are constants computed from spectroscopic data. From Ref. 5,  $\beta$  and  $E_\infty$  for hydrogen are  $1.85$  and  $7.55 \times 10^{-19}$  J, respectively, and  $2.34$  and  $1.05 \times 10^{-18}$  J, respectively, for oxygen. Unlike Lennard-Jones, the Morse potential is based on four parameters. The differences between the two potentials can be seen in Fig. 1. Figure 1 shows that the depth of the Morse potential compared to its long-range potential is far greater than that of Lennard-Jones. In addition, the Morse potential permits smaller separation distances between the atoms.

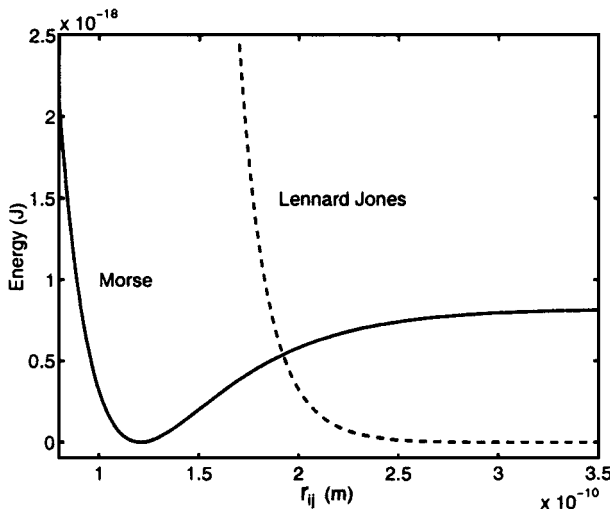


Fig. 1 Morse and Lennard-Jones potentials.

### Finite Difference Method

Once the potentials have been established, the equations of motion can be produced. One typical form of the equations of motion in MD is the Hamiltonian (see Ref. 6). The Hamiltonian is defined in terms of the Lagrangian  $L$  and a set of generalized coordinates  $q$

$$H(\mathbf{p}, \mathbf{q}) = \sum_k \dot{q}_k p_k - L(\mathbf{q}, \dot{\mathbf{q}}) \quad (4)$$

where  $p$  is given by

$$p_k = \frac{\partial L}{\partial \dot{q}_k} \quad (5)$$

and

$$\dot{q}_k = \frac{\partial H}{\partial p_k} \quad (6)$$

$$\dot{p}_k = -\frac{\partial H}{\partial q_k} \quad (7)$$

In terms of Cartesian coordinates, the equations of motion become

$$\dot{\mathbf{r}}_i = (\mathbf{p}_i/m_i) \quad (8)$$

$$\dot{\mathbf{p}}_i = -\nabla u = \mathbf{f}_i \quad (9)$$

These equations of motion must now be integrated to obtain the trajectories of the atoms. One of the most common finite difference methods is the velocity Verlet algorithm (see Ref. 7). This technique has the advantage of being third-order accurate even though it contains no third-order derivatives. The velocity Verlet is a two-step process. First, the position is advanced one time step and the velocity is advanced half of a time step:

$$\mathbf{r}(t + \Delta t) = \mathbf{r}(t) + \mathbf{v}(t)\Delta t + (\Delta t^2/2)\mathbf{a}(t) \quad (10)$$

$$\mathbf{v}[t + (\Delta t/2)] = \mathbf{v}(t) + (\Delta t/2)\mathbf{a}(t) \quad (11)$$

At this point, the forces are computed and velocity is advanced another half time step:

$$\mathbf{v}(t + \Delta t) = \mathbf{v}[t + (\Delta t/2)] + (\Delta t/2)\mathbf{a}(t + \Delta t) \quad (12)$$

This method offers simplicity and good stability for a relatively large time step. The velocity Verlet algorithm also has the advantage that it is relatively easy to program and requires little computer memory. These qualities are essential when modeling large numbers of atoms.

### Vibrational Energy Distribution

The first goal of this MD simulation was to model the vibrational energy distribution within a system of oxygen molecules. Vibrational energy is distributed in discrete energy levels according to the Boltzmann distribution (see Ref. 8),

$$\frac{N'^*}{N} = \frac{g_l e^{-\epsilon_v/kT}}{\sum g_l e^{-\epsilon_v/kT}} \quad (13)$$

where  $N'^*/N$  is the fraction of molecules in a particular level. For vibrational energy distribution, there is no degeneracy. This means that there is only one state per level or  $g_l$  is unity.

However, because vibrational energy increases in discrete increments, a relationship must be formed between the quantum energy levels and the vibrational energy. This relationship is given by

$$\epsilon_v = \omega_e(v + 0.5) - x_e\omega_e(v + 0.5)^2 - 0.5\omega_e + 0.25x_e\omega_e \quad (14)$$

where  $x_e\omega_e$  is the first anharmonic correction.<sup>9</sup>

In contrast, the MD code outputs vibrational energy that must then be converted to discrete quantum levels by solving Eq. (14) for  $v$ . This operation is performed on every molecule at every time

step. One further complication is that  $\nu$  must be an integer. Simply truncating  $\nu$  is the most efficient way to convert it from a real number to an integer. Truncation ensures that the zero energy level bin is equal in size to the other bins. The last step is to count the number of molecules in each energy level. At this point, the results can be compared to kinetic theory.

### Reactions

The second part of this investigation focuses on modeling the dissociation and recombination of a single molecular species, in this case, either hydrogen or oxygen.

#### Kinetic Theory

According to kinetic theory, dissociation occurs when a second body impacts a molecule at a sufficient energy level. In the case of a single-species system, only one type of atom is present, which means the second body can be either another molecule or another atom. If the impact occurs with an energy greater than the dissociation energy of the molecule, the molecule dissociates.

Similarly, recombination is modeled as a three-body reaction. The first two bodies are atoms, and the third is another atom or molecule. When the three bodies collide, energy is released as the two atoms combine. This energy is then transferred to the third body in the form of translational motion. This type of reaction is less common than dissociation because it involves the collision of three bodies. Hence, an equation can be formed to describe the degree of dissociation in a system of diatomic molecules as a function of time<sup>8</sup>:

$$\frac{d\alpha}{dt} = \frac{C_f}{m} T^n \rho \left[ (1 - \alpha) e^{-\theta_d/T} - \frac{\rho}{\rho_d} \alpha^2 \right] \quad (15)$$

In this equation,  $C_f$  and  $n$  are experimentally determined rate parameters. In addition, a similar equation can be formed for the equilibrium degree of dissociation:

$$\alpha^*/(1 - \alpha^*) = \exp(-\Theta_d/T)/\rho \left\{ m(\pi mk/h^2)^{\frac{3}{2}} \times \Theta_r \sqrt{T} [1 - \exp(-\Theta_v/T)] (Q_{cl}^d)^2 / Q_{cl}^{aa} \right\} \quad (16)$$

In this equation,  $\Theta_d$  is the characteristic temperature of dissociation,  $\Theta_r$  is the rotational characteristic temperature, and  $\Theta_v$  is the vibrational characteristic temperature. However, this is a very complicated expression and can be simplified by the Lighthill approximation (see Ref. 8). Lighthill found that the value of the bracketed expression remained relatively constant and could be given by  $\rho_d$ , the characteristic density. This simplifies Eq. (16) to the form

$$\alpha^*/(1 - \alpha^*) = [\exp(-\Theta_d/T)/\rho] \rho_d \quad (17)$$

#### MD

Unfortunately, it is not possible to apply this technique to an MD simulation that uses atomic potentials because there are no discrete collisions. The distance between atoms never actually goes to zero because this would cause an infinite repulsive potential. Also, due to the high densities studied here, at any instant of time a particular atom, whether combined in a molecule or not, is experiencing forces from up to 20 neighboring atoms. Therefore, another technique must be used to simulate dissociation and recombination reactions.

The method chosen for this MD code was curve hopping.<sup>10-12</sup> The molecules acquire or lose vibrational energy due to force interactions with neighboring atoms and molecules. Dissociation takes place when the potential between two atoms of an oxygen molecule exceeds some critical value. This is analogous to the vibrational energy of the molecule exceeding a critical value. The point at which this occurs is relatively ambiguous because it is difficult to define explicitly the point on the Morse potential curve<sup>5</sup> where the molecule dissociates. Therefore, in this simulation, a molecule is said to dissociate when the potential between the two atoms reaches 96% of the dissociation energy. This value was chosen because it produced suitable agreement with kinetic theory. However, the results were only slightly affected by varying this ratio between 90 and 99%.

As dissociation occurs, the atoms jump from the Morse<sup>5</sup> to the Lennard-Jones potential, hence, curve hopping.

Recombination of atoms is performed in the opposite manner. When the potential between two dissociated atoms decreases below 0.5 kT, the atoms combine to form an oxygen molecule.<sup>11</sup> When recombination occurs the potential between the two atoms is switched from the Lennard-Jones to the Morse potential.<sup>5</sup>

Both recombination and dissociation require a change of potential surface for the two atoms involved in the process. When this switch occurs, there is a jump in the potential energy of the constituent atoms. To account for this, the atoms' velocities are scaled to adjust their kinetic energy to match the change in potential so that the total energy of the system remains constant.<sup>10</sup> Subsequently, as the atoms move with their new velocities, they affect their neighbors. In the case of recombination, the energy released by the creation of an oxygen molecule is transferred to the surrounding atoms by this process. Therefore, no third body is required for recombination to occur.

### MD Simulation

Two different types of codes are used in this MD simulation. The first is a vibrational energy distribution code that only models atomic vibration and does not allow the molecules to dissociate. This program is used to compute the Boltzmann distribution. The second code is a reaction code that is very similar to the vibrational energy distribution program. The only major difference is that the reaction code allows dissociation and recombination. This is accomplished by updating an array that specifies which atoms are connected. The reaction code is used to compute the degree and rate of dissociation in the system. Both hydrogen and oxygen were simulated individually by the two codes.

In each case, the simulation begins with the entire system as molecular species and arranged in a face-centered cubic lattice with the intermolecular spacing chosen to give the desired system density. A cubic environment is utilized, and periodic boundary conditions are imposed. When computing the vibrational energy distribution, 256 molecules were used. However, only 108 molecules were present in the single-species reaction simulation. This reduction in atoms vastly increased the speed of the code that was necessary because of the relatively long time period required for the system to achieve equilibrium. All of these codes use a 1 femtosecond (fs) time step for oxygen and a 0.2 fs time step for hydrogen. Such small time steps are required to model accurately the high-frequency vibrations of the atoms. Standard MD codes use time steps an order of magnitude larger.

In addition, these programs employ a variety of techniques that greatly increase the performance of the code. The first of these methods reduces the number of force calculations by limiting the range of the Lennard-Jones potential. This technique is valid because the intermolecular potential becomes very small at atomic separation distances of only a few diameters. For this simulation, a cutoff radius of  $2.5\sigma$  was selected. There is a resulting jump in potential energy as an atom crosses this radius, but it is usually very small. In addition, because the force that atom 1 exerts on atom 2 is equal to the force that atom 2 exerts on atom 1, only one force calculation needs to be performed for both situations.

Four identical versions of the vibrational energy distribution code were submitted to four processors of COCOA. The temperature and density of the systems would be the same, but the initial velocities of the atoms were chosen at random. This caused each case to produce slightly different results that, when averaged, reduced fluctuations in the vibrational energy distribution curve. COCOA is a collection of 25 dual processor Pentium® II computers linked together by fast Ethernet.<sup>13</sup> A 20,000 time step run would typically take about 2 h to complete. In the case of the reacting gas, eight identical codes were executed on COCOA with varying initial conditions. In the case of hydrogen,  $45 \times 10^6$  time steps were used. This code would take about 27 h to run. In the case of oxygen,  $70 \times 10^6$  time steps were used, which took about 48 h to run. This means that the hydrogen code ran at  $1.67 \times 10^6$  time steps per hour, whereas the oxygen code ran at  $1.45 \times 10^6$  time steps per hour. The difference between the

two codes was the number of linked list cells used. In the case of hydrogen, the density of the system allowed nine cells per dimension to be used, whereas the oxygen case only allowed eight cells per dimension. This is a perfect example of the effect of linked list cells on the performance of an MD code.

## Results and Discussion

The first goal of this investigation was to determine the vibrational energy distribution in a system of molecules. Simulations were run at a variety of temperatures using either hydrogen or oxygen. In all cases, 256 molecules were present, and the code was executed for 20,000 time steps. Because the distribution is averaged over time, the more time steps performed, the smaller the statistical fluctuations are.

Figure 2 shows the vibrational energy distribution of oxygen calculated using MD compared to the Boltzmann distribution computed for both harmonic and anharmonic interatomic potentials at a temperature of 1942 K. It shows excellent agreement between the MD code and the Boltzmann distribution. The plot is given in terms of the normalized fraction of molecules relative to the zero vibrational energy level. Because this MD simulation utilizes the Morse potential,<sup>5</sup> the computational points should lie on the anharmonic distribution. The results show a small deviation from the theoretical curve at higher energy levels, which could be improved by increasing the number of time steps and increasing the number of molecules in the system.

Figure 3 shows the vibrational energy distribution of hydrogen molecules calculated using MD compared to the Boltzmann distribution computed for both harmonic and anharmonic interatomic potentials at a temperature of 3935 K. Excellent agreement can be seen between the MD results and the Boltzmann distribution. However, the MD compares better with the harmonic Boltzmann distribution than the anharmonic distribution. This is unexpected because the Morse potential<sup>5</sup> is an anharmonic potential. In addition, as indicated by the high temperature at which this simulation was run, hydrogen molecules require much greater energy to reach higher energy levels. It is felt that the discrepancy between the calculated hydrogen vibrational energy distribution and the anharmonic Boltzmann distribution is due to the small number of molecules (256) used in the simulation, where a change in the energy level of one molecule represents a change in the normalized fraction of 0.004.

The second part of this investigation examined the dissociation and recombination reactions in a system of atomic and molecular species. Because of the large number of time steps required, only 108 molecules were used with the system volume reduced accordingly. In addition, only high-pressure and high-temperature cases were examined to minimize the time required for the system to

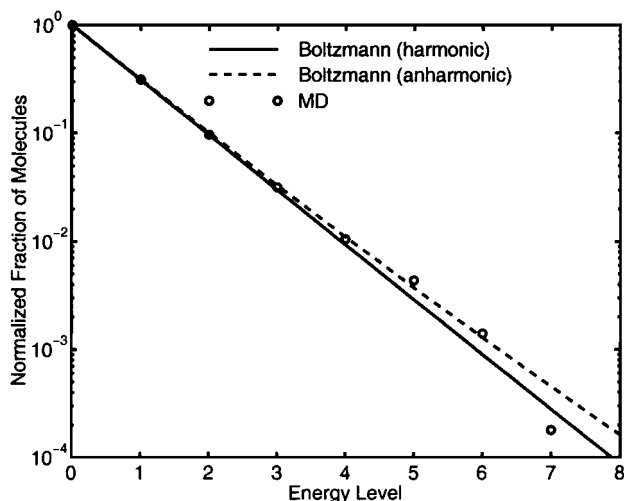


Fig. 2 Vibrational energy distribution of oxygen molecules calculated using MD compared to Boltzmann distribution for both harmonic and anharmonic interatomic potentials,  $T = 1942$  K.

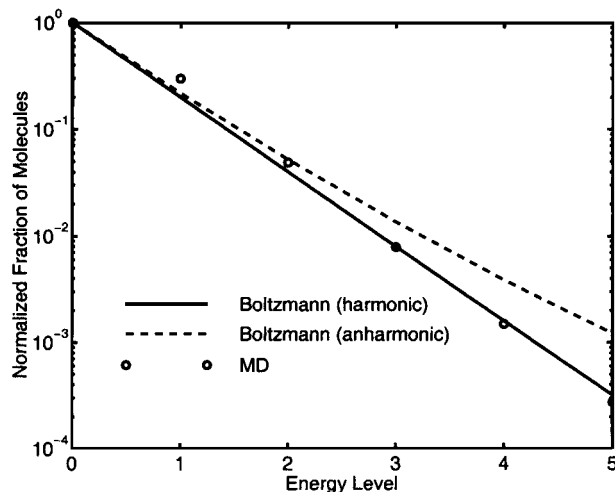


Fig. 3 Vibrational energy distribution of hydrogen molecules calculated using MD compared to Boltzmann distribution for both harmonic and anharmonic interatomic potentials,  $T = 3935$  K.

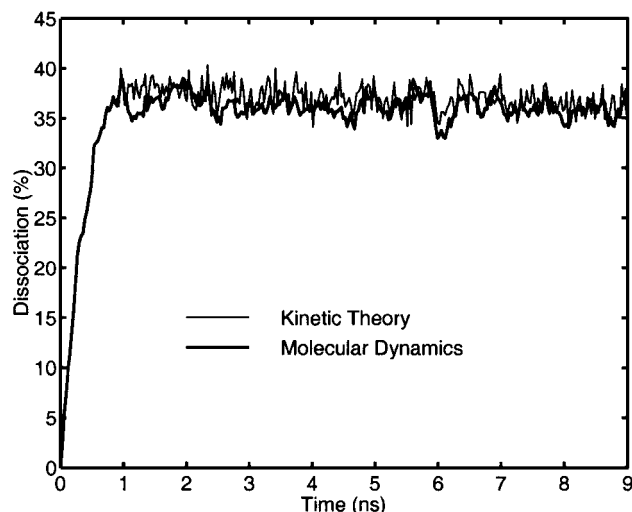


Fig. 4 MD computation of the degree of dissociation of hydrogen at pressure of 35 MPa and mean temperature of 5860 K compared to equilibrium kinetic theory.

achieve equilibrium. An initial number of molecules, volume, and temperature are specified. The volume and number of atoms are kept constant, and the temperature is allowed to vary as the simulation proceeds. Pressure is then calculated from the perfect gas law using the calculated temperature and composition (degree of dissociation). Different pressures are simulated by using different simulation volumes. Figure 4 shows the MD simulation of the degree of dissociation of hydrogen at a pressure of 35 MPa and a mean temperature of 5860 K compared to kinetic theory.

In the Fig. 4 plot, the thick line represents the MD data, whereas the thin line represents kinetic theory. As can be seen from the plot, the MD simulation begins with no dissociation. The system reaches equilibrium quickly and is then compared to equilibrium kinetic theory. The kinetic theory fluctuates based on fluctuations in temperature. The Lennard-Jones parameters chosen for this simulation were  $\sigma = 2.7 \times 10^{-10}$  m and  $\epsilon = 4.0 \times 10^{-22}$  J. This plot demonstrates good agreement between MD simulation and kinetic theory. Simulations were also conducted at the same density but at two higher temperatures, 6000 and 6180 K, with the same agreement with kinetic theory.

Figure 5 shows the temperature fluctuations that occur during the simulation. The Fig. 5 plot clearly shows the initial rise in temperature that occurs when the molecules are dissociating. This

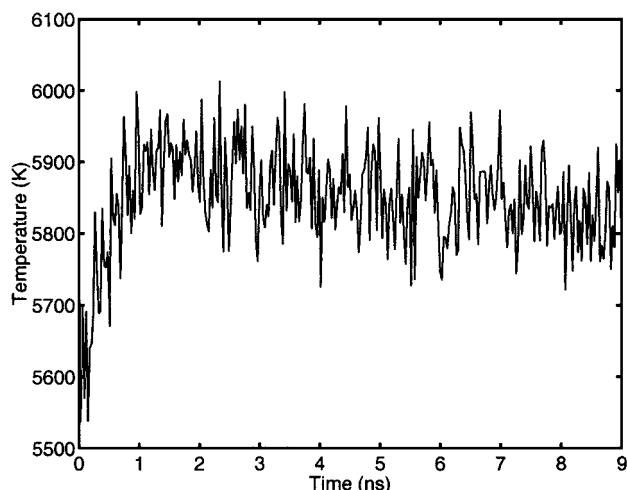


Fig. 5 Temperature fluctuation during the simulation of hydrogen dissociation at 35 MPa and 5860 K.

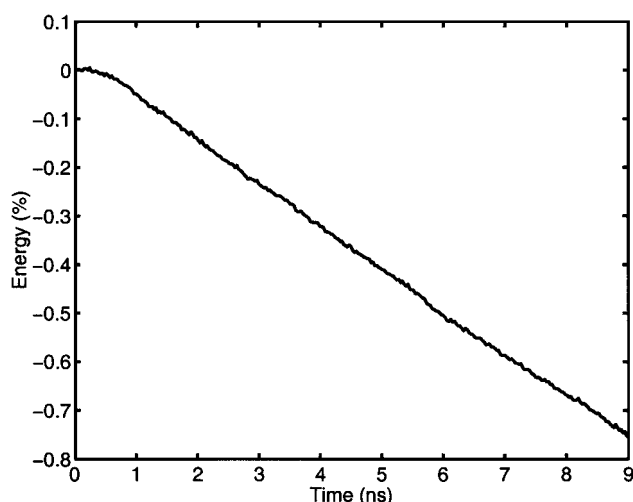


Fig. 6 Energy drop during simulation of hydrogen dissociation at 35 MPa and 5860 K.

temperature rise is caused by the breaking of chemical bonds. When a bond breaks, the chemical potential energy of the bond is converted to kinetic energy in the form of increased atomic motion. This, naturally, increases the temperature of the system. Also note the high-frequency fluctuations in temperature that occur when the system reaches equilibrium. The temperature can vary by up to 200 K. This temperature fluctuation is caused by the large number of molecules that are dissociating and recombining.

Figure 6 shows the energy drop that occurs during the simulation. The drop in energy takes place over a relatively long span of  $45 \times 10^6$  time steps. In this period, the energy drops by roughly 0.75%. This small percentage drop is not a significant loss in energy for an MD simulation extending over that many time steps<sup>4</sup> and does not adversely affect the system. However, this loss of energy cannot be remedied because of the nature of the dissociation code. When a molecule dissociates, the energy released is transferred into the resulting atoms. This increase in kinetic energy causes the atoms to increase dramatically their velocity. Frequently, the velocity of the atoms exceeds the maximum value allowed by the time step. The result is a loss of total energy in the system. This problem could be solved by decreasing the time step, but that would cause the code to run slower.

In addition to the hydrogen simulations, MD simulations of the dissociation of oxygen were performed. Similar to the hydrogen simulations, three cases were run at various temperatures and constant density. Furthermore, because oxygen is one of the main components of the atmosphere, its dissociation has been more closely

examined by experimenters and dissociation rate data can be found in the literature. Therefore, the MD code cannot only be compared to the theoretical equilibrium degree of dissociation, but also to the kinetic theory rate equation. The Lennard-Jones parameters chosen for this run were  $\sigma = 3.0 \times 10^{-10}$  m and  $\varepsilon = 9.0 \times 10^{-22}$  J. Figure 7 shows the MD results compared to the equilibrium degree of dissociation of oxygen at 46 MPa and a mean temperature of 6110 K. Again, there is excellent agreement between the MD results and kinetic theory. Just as in the hydrogen runs, there is an initial temperature rise as dissociation occurs. However, the system of oxygen takes longer to reach equilibrium due to the larger particle masses. Simulations were also conducted at 5690 and 6240 K with the same good agreement with kinetic theory.

According to kinetic theory, Eq. (15), the rate of dissociation is based on two parameters  $C_f$  and  $n$ . Note that  $n$  is very difficult to measure experimentally due to the limitations of the test apparatus, principally shock tubes.<sup>14</sup> Therefore, most experimentalists arbitrarily chose  $n$  to be  $-1.5$  for oxygen and experimentally determine  $C_f$ . In addition,  $C_f$  can vary up to 50%. Therefore, the experimentally determined  $C_f$  was used (Ref. 15),  $1.97 \times 10^{21} \text{ cm}^3 \text{ mole}^{-1} \text{ s}^{-1} \text{ K}^{1.6}$ , and  $n$  was chosen to be  $-1.6$ , which gave the best match to the MD results. However, there is very little difference between this value and the one arbitrarily selected for experiments. Figure 8 shows the MD results compared to the kinetic theory rate equation for the same conditions as Fig. 7. It can be seen that the rate of dissociation calculated via MD for this dilute gas case compares very well with that predicted by kinetic theory.

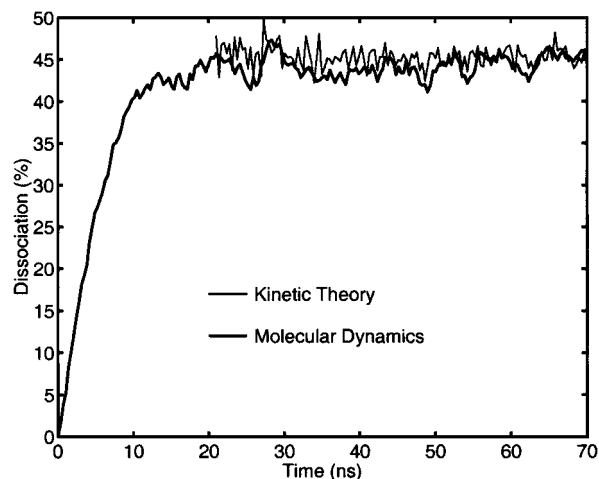


Fig. 7 MD computation of degree of dissociation of oxygen at 46 MPa and mean temperature of 6110 K compared to equilibrium kinetic theory.

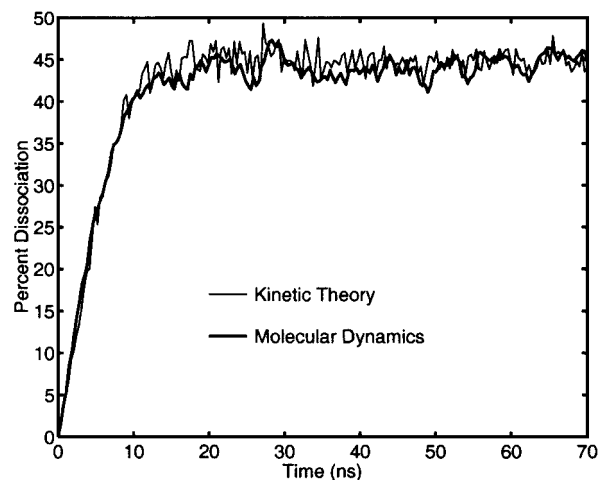


Fig. 8 MD computation of degree of dissociation of oxygen at 46 MPa and mean temperature of 6110 K compared to theoretical rate of dissociation.

## Conclusions

The vibrational energy distribution and dissociation/recombination reactions of hydrogen and oxygen were examined by MD simulations. Results of the vibrational energy distribution studies showed excellent agreement with the Boltzmann distribution. Both the rate of dissociation and the equilibrium degree of dissociation also compared well to kinetic theory. This investigation has demonstrated that simple chemical reactions can be modeled by MD.

However, this project is only the first step in modeling chemical reactions by the curve hopping method of MD. The simulations performed in this investigation only contained a few hundred atoms. Future simulations should be considerably larger. This could be accomplished without diminished performance by parallelization of the code. In addition, water, which was not modeled in this program, should be included in future simulations. When water is included, the hydrogen/oxygen combustion process can be completely modeled by MD.

## Acknowledgment

This work was supported by the Air Force Office of Scientific Research under Grant F49620-97-1-0128.

## References

- <sup>1</sup>Kaltz, T. L., Long, L. N., Micci, M. M., and Little, J. K., "Supercritical Vaporization of Liquid Oxygen Droplets Using Molecular Dynamics," *Combustion Science and Technology*, Vol. 136, Nos. 1-6, 1998, pp. 279-301.
- <sup>2</sup>Nwobi, O. C., Long, L. N., and Micci, M. M., "Molecular Dynamics Studies of Properties of Supercritical Fluids," *Journal of Thermophysics and Heat Transfer*, Vol. 12, No. 3, 1998, pp. 322-327.

- <sup>3</sup>Nwobi, O. C., Long, L. N., and Micci, M. M., "Molecular Dynamics Studies of Thermophysical Properties of Supercritical Ethylene," *Journal of Thermophysics and Heat Transfer*, Vol. 13, No. 3, 1999, pp. 351-354.
- <sup>4</sup>Rapaport, D. C., *The Art of Molecular Dynamics Simulation*, 1st ed., Cambridge Univ. Press, Cambridge, England, U.K., 1995, p. 13.
- <sup>5</sup>Morse, P. M., "Diatomic Molecules According to the Wave Mechanics. II. Vibrational Levels," *Physical Review*, Vol. 34, July 1929, pp. 57-64.
- <sup>6</sup>Haile, J. M., *Molecular Dynamics Simulation: Elementary Methods*, 1st ed., Wiley, New York, 1992, pp. 40-43.
- <sup>7</sup>Allen, M. P., and Tildesley, D. J., *Computer Simulation of Liquids*, 1st ed., Clarendon, Oxford, England, U.K., 1987, pp. 81, 82.
- <sup>8</sup>Vincenti, W. G., and Kruger, C. H., *Introduction to Physical Gas Dynamics*, Krieger, Malabar, FL, 1986, p. 110.
- <sup>9</sup>Suchard, S. N., and Melzer, J. E., *Spectroscopic Data, Volume 2: Homonuclear Diatomic Molecules*, Aerospace Corp., Los Angeles, 1976, p. 5.
- <sup>10</sup>Liu, Q., Wang, J., and Zewail, A. H., "Solvation Ultrafast Dynamics of Reactions. 10. Molecular Dynamics Studies of Dissociation, Recombination and Coherence," *Journal of Physical Chemistry*, Vol. 99, No. 29, 1995, pp. 11321-11332.
- <sup>11</sup>Song, T. T., Hwang, Y. S., and Su, T. M., "Recombination Reactions of Atomic Chlorine in Compressed Gases. 3. Molecular Dynamics and Smoluchowski Equation Studies with Argon Pressure up to 6 kbar," *Journal of Physical Chemistry*, Vol. 101, No. 21, 1997, pp. 3860-3870.
- <sup>12</sup>Amar, F. G., and Berne, B. J., "Reaction Dynamics and the Cage Effect in Microclusters of Br<sub>2</sub>Ar<sub>n</sub>," *Journal of Physical Chemistry*, Vol. 88, No. 26, 1984, pp. 6720-6727.
- <sup>13</sup>Modi, A., and Long, L. N., "Unsteady Separated Flow Simulations using a Cluster of Workstations," AIAA Paper 2000-0272, Jan. 2000.
- <sup>14</sup>Park, C., "Two-Temperature Interpretation of Dissociation Rate Data for N<sub>2</sub> and O<sub>2</sub>," AIAA Paper 88-0458, Jan. 1988.
- <sup>15</sup>Byron, S. R., "Measurement of the Rate of Dissociation of Oxygen," *Journal of Chemical Physics*, Vol. 30, No. 6, 1959, pp. 1380-1392.